Available online at www.sciencedirect.com
SCIENCE DIRECT®

Nuclear Science and Techniques, Vol.17, No.1 (2006) 53–60

NUCLEAR
SCIENCE
AND
TECHNIQUES

Simulation of chemical kinetics in sodium-concrete interactions

ZHANG Bin * ZHU Ji-Zhou SHAN Jian-Qiang WANG Xue-Rong

(Nuclear Safety Group, Nuclear Engineering Department, Xi'an Jiaotong University, Xi'an 710049, China)

Abstract Sodium-concrete interaction is a key safety-related issue in safety analysis of liquid metal cooled fast breeder reactors (LMFBRs). The chemical kinetics model is a key component of the sodium-concrete interaction model. Conservation equations integrated in sodium-concrete interaction model cannot be solved without a set of relationships that couple the equations together, and this may be done by the chemical kinetics model. Simultaneously, simulation of chemical kinetics is difficult due to complexity of the mechanism of chemical reactions between sodium and concrete. This paper describes the chemical kinetics simulation under some hypotheses. The chemical kinetics model was integrated with the conservation equations to form a computer code. Penetration depth, penetration rate, hydrogen flux, reaction heat, etc. can be provided by this code. Theoretical models and computational procedure were recounted in detail. Good agreements of an overall transient behavior were obtained in a series of sodium-concrete interaction experiment analysis. Comparison between analytical and experimental results showed that the chemical kinetics model presented in this paper was creditable and reasonable for simulating the sodium-concrete interactions.

Key words LMFBRs, Sodium-concrete interactions, Chemical kinetics.

CLC numbers TL343, TL364

1 Introduction

In liquid metal cooled fast breeder reactors (LMFBRs), direct contact between sodium and concrete is unavoidable, especially in severe accidents. Due to its high chemical reactivity, sodium tends to react with concrete violently, resulting in release of hydrogen and heat in increased quantities. The integrality of the containment will be challenged. In other words, sodium-concrete interaction becomes a key issue in safety analysis of LMFBRs.

Usually, a sodium-concrete interaction model consists of a series of conservation equations and chemical kinetic equations. In conservation equations, energy equation is solved for the temperature distribution. A pressure distribution is evaluated based upon temperature and the air-water-void distribution. The velocities of air and water are calculated from Darcy's law, i.e. the momentum equations. The continuity equations for air and water are updated with the new velocities calculated from above. However, the equations described above cannot be solved without a set of relationships that couple the equations together. The required relationships will be discussed in chemical kinetics models.

2 Mechanism of chemical reactions

The detailed processes of chemical reactions between sodium and concrete vary according to the type of the concrete. Hence, it is difficult to sum up all kinds of sodium-concrete interactions. However, we can divide the whole reaction into two periods, namely, the first is for sodium-water reaction, and the second is for sodium-solid reaction. When hot sodium is rapidly placed on the concrete with ambient temperature,

---

Supported by National Natural Science Foundation of China (Grant No. 19785002)

* Corresponding author. E-mail address: binzhang@mail.xjtu.edu.cn

Received date: 2005-03-24

water is immediately released from the concrete surface and reacts with sodium to form hydrogen, sodium hydride, and sodium hydroxide. During this period, the ablation of sodium can be neglected. Then sodium reacts with solid. Reaction between sodium and solid includes the reaction between NaOH and concrete. Further, a threshold temperature exists below which the sodium-solid reaction does not occur at a significant rate.

The following is a sketch figure of sodium and basalt concrete interaction[1]. There is a Primary Reaction Zone in the figure, viz. sodium-water interaction plane. On each side of this plane there is one zone, viz. Zone 1 and Zone 2, as shown in Fig.1.

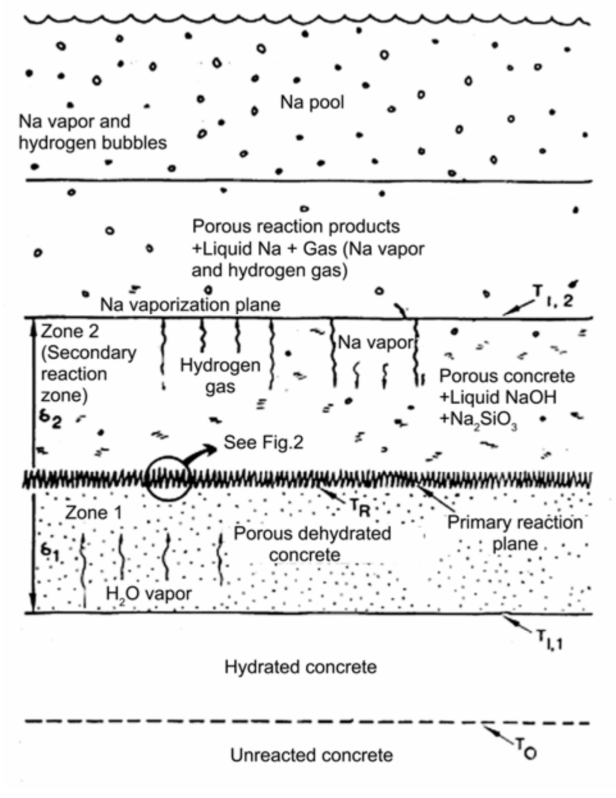

Fig. 1 Sketch figure of sodium-concrete interaction.

Zone 1 is below the Primary Reaction Zone. Water vapor in concrete is released and diffused to Primary Reaction Zone driven by the vapor pressure due to heat conduction from "dry zone" of Zone 1 to "wet zone". Water vapor comes from evaporable water and chemically bound water in the "wet zone" which is below Zone 1.

Zone 2 is above the Primary Reaction Zone. In this zone, sodium is transported downward to reaction zone turbulently by diffusion. At the boundary of Zone 2 and porous reaction product layer, sodium liquid is heated to produce sodium vapor partially.

At reaction plane sodium vapor coming from Zone 2 reacts intensively with water vapor coming from Zone 1, thereby producing NaOH and hydrogen. However, temperatures in the reaction zone are well below the boiling point of NaOH (b.p. = 1700K). This causes NaOH to condense rapidly in the region above Primary Reaction Zone. But because of the limited penetration rate of Primary Reaction Zone through concrete, the region of NaOH distributes equally, as depicted schematically in Fig.2[2].

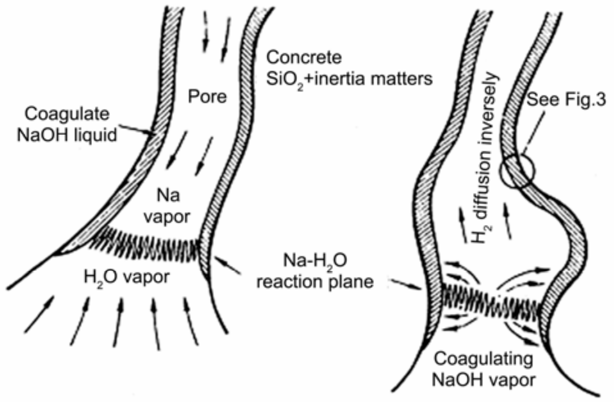

Fig. 2 Local figure of porous dry zone.

The region of NaOH reacts secondly in Zone 2 and Na_2SiO_3 and water vapor are produced, as depicted schematically in Fig.3. Water vapor produced will react with sodium of Zone 2, and ultimately producing NaOH and hydrogen.

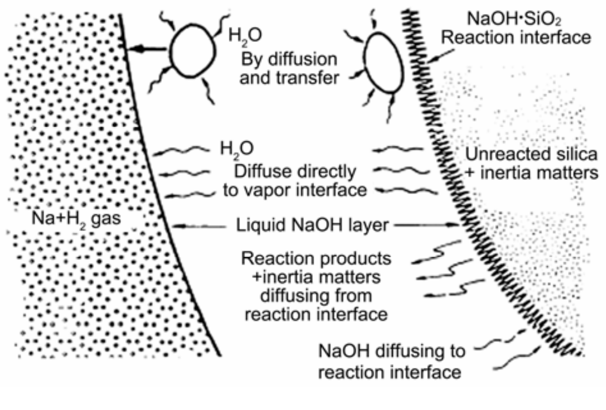

Fig. 3 Schematic diagram of coagulate NaOH liquid layer.

Hydrogen produced by the reaction exists in Zone 1 as the form of static state diffusion gas. But in Zone 2 hydrogen exists as the form of diffusion gas and diffuses upward. In the porous reaction product layer upon Zone 2, hydrogen lies with sodium liquid in saturated heat balance state. Ultimately, hydrogen and sodium come into being saturated bubbles and escape from the sodium-concrete system, entering into the containment.

3 Chemical kinetics equations

Chemical kinetics equations depend on the following hypotheses.

1. Secondary reaction of NaOH-SiO_2 just takes place on the surface of gravel.
2. As reaction is going on, the sizes of sand and gravel diminish gradually.
3. When cement that glues concrete together meets coagulate NaOH, it dissolves immediately and forms reactant slurry.
4. Relative to the velocity of chemical reaction, diffusion of NaOH to the surface of reaction can be neglected.
5. In reactant slurry, the inert components of sand, gravel and cement slurry just dilute NaOH, having no other influence on the reaction.
6. Water produced in secondary reaction reacts immediately with sodium, produces excess NaOH and hydrogen gas. Hence, we cannot take diffusion of water, sodium and hydrogen gas into account.
7. Penetration rate is independent of size of granule.

There are two basic equations for the chemical kinetics model, namely:

$$V = \lambda K \exp\left(-E/RT\right) \tag{1}$$

where V is penetration rate at reaction interface, i.e. the velocity of dry zone concrete entering into reaction zone; λ is chemical reaction coefficient of sodium hydroxide; R is gas constant; T is local temperature; K and E are constants measured in experiments: $K = 3.5\times10^{-2}$ m/s; and $E = 7.607\times10^{4}$ J/mol.

Equation (1) is an empirical equation obtained from experiments.

$$\frac{\mathrm{d}\alpha_s}{\mathrm{d}t} = VA_s \tag{2}$$

where α_s is mass fraction of eroded matter and A_s is surface area of every voluminal unit of reactant.

Uniting Eq. (1) and Eq. (2) gives

$$\frac{\mathrm{d}\alpha_s}{\mathrm{d}t} = A_s \lambda K \exp\left(-E/RT\right) \tag{3}$$

Due to hypothesis (6), secondary reaction equation is as follows:

$$\mathrm{Na_g + NaOH_l + SiO_{2s}} + x\mathrm{I_s} \rightarrow \mathrm{Na_2SiO_{3l}} + x\mathrm{I_l} + \frac{1}{2}\mathrm{H_{2g}} \tag{4}$$

where I refers to inert matter.

Multiplying $\bar{\rho}_{\mathrm{Si}}$, molar density of silica, on both sides of Eq. (3), and using Eq. (4) we obtain

$$\frac{\mathrm{d}\bar{\rho}_{\mathrm{NaOH}}}{\mathrm{d}t} = A_s \lambda \bar{\rho}_{\mathrm{Si}} K \exp\left(-E/RT\right) \tag{5}$$

where $\bar{\rho}_{\mathrm{NaOH}}$ is molar density of NaOH liquid. Integrating Eq. (5), we can find that both initial density and final density of NaOH relate with f, consuming fraction of NaOH.

Before integrating Eq. (5), we should acquire the values of the following parameters: λ, chemical reaction coefficient, and A_s.

3.1 Chemical reaction coefficient of NaOH

Chemical reaction coefficient of NaOH is molar fraction of NaOH in liquid reactant slurry. Liquid slurry consists of NaOH, Na_2SiO_3 and inert matters. According to Eq. (4), when 1 molar NaOH participates reaction, 1 molar Na_2SiO_3 and X molar inert matters will be produced. Inert matters consists of calcium oxide and alumina. The initial density of them is X^0. So,

$$\lambda = \frac{\bar{\rho}_{\mathrm{NaOH}}}{\bar{\rho}_{\mathrm{NaOH}} + \left(\bar{\rho}^0_{\mathrm{NaOH}} - \bar{\rho}_{\mathrm{NaOH}}\right)\left(1 + X\right) + X^0} \tag{6}$$

Eq. (6) is an expression of chemical reaction coefficient of NaOH in the whole liquid, while Eq. (5) gives reaction velocity of NaOH on the surface of sand and gravel. Thus, λ in Eq. (5) is chemical reaction coefficient on the surface of sand and gravel, and not in the whole liquid. To keep it simple, diffusion of NaOH is neglected and Eq. (6) is used as the expression of chemical reaction factor on the surface of sand and gravel.

3.2 Surface area in every voluminal unit of reactant

Surface area in every voluminal unit of reactant is the sum of the surface area of both sand and gravel in every voluminal unit. In order to get the expression of surface area, we define a distribution function $\mathrm{d}N/\mathrm{d}R$, which stands for total amount of sand and gravel between R and $(R+\mathrm{d}R)$ in every voluminal unit. Using this definition and assuming all granules to be global give the volume of all granules (supposing the radius of all granules is R):

$$\mathrm{Volume} = \int_0^R \frac{4}{3}\pi R^3 \frac{\mathrm{d}N}{\mathrm{d}R}\mathrm{d}R \tag{7}$$

Supposing that $\mathrm{d}N/\mathrm{d}R$ consists of two parts: distribution of sand and distribution of gravel, we have

$$\frac{\mathrm{d}N}{\mathrm{d}R} = \frac{\mathrm{d}N_\mathrm{s}}{\mathrm{d}R} + \frac{\mathrm{d}N_\mathrm{g}}{\mathrm{d}R} \tag{8}$$

$$\frac{\mathrm{d}N_\mathrm{s}}{\mathrm{d}R} = A_1 \exp\left[-\left(R-R_\mathrm{s}\right)^2 A_2^2\right] \tag{9}$$

$$\frac{\mathrm{d}N_\mathrm{g}}{\mathrm{d}R} = A_3 \exp\left[-\left(R-R_g\right)^2 A_4^2\right] \tag{10}$$

where N_s is the amount of sand and N_g is the amount of gravel, A_i, R_s and R_g are all constants denoting character of distribution.

To basalt concrete, there are

$$\begin{aligned} A_1 &= 2.46\times10^{12}\ \mathrm{m}^{-3} \\ R_\mathrm{s} &= 5\times10^{-5}\ \mathrm{m} \\ A_2 &= 2.2\times10^{3}\ \mathrm{m}^{-3} \\ A_3 &= 4.22\times10^{8}\ \mathrm{m}^{-3} \\ R_\mathrm{g} &= 3\times10^{-3}\ \mathrm{m} \\ A_4 &= 400\,\mathrm{m}^{-3} \end{aligned} \tag{11}$$

R_s and R_g are functions of time:

$$R_\mathrm{s} = R_\mathrm{s}^0 - \delta_\mathrm{r}(t) \tag{12}$$

$$R_\mathrm{g} = R_\mathrm{g}^0 - \delta_\mathrm{r}(t) \tag{13}$$

where δ_r is corrosion radium of sand and gravel, R_s^0 is the initial value of R_s and R_g^0 is the initial value of R_g.

Using Eq. (7) to Eq. (13) gives

$$A_\mathrm{s}(t) = \int_0^{R_{\max}} 4\pi R^2 \frac{\mathrm{d}N}{\mathrm{d}R}(t)\mathrm{d}R \tag{14}$$

4 Computational procedure

This is a non-linear problem. Iteration technique[3] is appropriate to solve the chemical kinetics model. The following is the flow of calculation for a certain time.

1. Supposing chemical reaction coefficient, $\lambda(\eta)$, equals 1, and depth of Zone 2, δ, is a certain value, calculate $\dfrac{\delta}{V} = \dfrac{\delta^2}{\delta\cdot V}$;
2. Calculate $V(\eta) = \lambda(\eta) K \exp\left[-E/RT(\eta)\right]$. where $T(\eta)$ can be acquired from conservation equations;
3. Calculate the total changes of radium at any position: $\delta_r(\eta) = \dfrac{\delta}{V}\displaystyle\int_0^\eta V(\eta)\mathrm{d}\eta$;
4. Calculate the total surface
$$A_\mathrm{s}(\eta) = \int_0^{R_{\max}-\delta_r(t)} 4\pi R^2 \frac{\mathrm{d}N}{\mathrm{d}R}\mathrm{d}R,$$
where
$$\frac{\mathrm{d}N}{\mathrm{d}R} = A_1 \exp\left\{-A_2^2\left[R-\left(R_\mathrm{s}-\delta_r(\eta)\right)\right]^2\right\} + A_3 \exp\left\{-A_4^2\left[R-\left(R_g-\delta_r(\eta)\right)\right]^2\right\};$$
5. Integrate Eq. (5) and save the result of integral:
$$g(\eta) = \int_0^\eta \frac{\bar{\rho}_\mathrm{Si}}{\bar{\rho}_\mathrm{NaOH}} A_\mathrm{s}(t)\lambda(\eta) K \exp\left[-E/RT(\eta)\right]\mathrm{d}\eta;$$
6. Calculate $\dfrac{\delta}{V}$ using the following equation:
$$\left(\frac{\delta}{V}\right)^* = \frac{f(1-f)}{g(\eta=1)};$$
7. Calculate the density of NaOH:
$$\bar{\rho}_\mathrm{NaOH} = \bar{\rho}_\mathrm{NaOH}^0\left(1-\left(\frac{\delta}{V}\right)^* g(\eta)\right);$$
8. Calculate chemical reaction coefficient λ:
$$\lambda(\eta) = \frac{\bar{\rho}_\mathrm{NaOH}}{\bar{\rho}_\mathrm{NaOH} + \left(\bar{\rho}_\mathrm{NaOH}^0 - \bar{\rho}_\mathrm{NaOH}\right)\left(X+1\right) + X^0};$$
9. Convergence judge:

Compare $\left(\frac{\delta}{V}\right)^{*}$, calculated in step 6, with $\left(\frac{\delta}{V}\right)$, calculated in step 1. If they are not the same, then let $\left(\frac{\delta}{V}\right)=\left(\frac{\delta}{V}\right)^{*}$, then $\delta=\left(\frac{\delta}{V}V\cdot\delta\right)^{1/2}$, and $V=\frac{V\cdot\delta}{\delta}$. Go back to step 2, repeat the following steps until the two parameters are the same. If they are similar, then proceed with the next time.

5 Validation of chemical kinetics model

It is impossible to validate the above chemical kinetics model separately. The above model is integrated with the conservation equations to form a program. Good agreement between the results of the program and the experiment has shown the rationality and veracity of the above chemical kinetics model.

In the 70's and 80's of last century, Sandia National Laboratory and Hanford Engineering Development Laboratory did many experiments upon sodium concrete interactions. The cases applied in this paper are derived mainly from their work.

5.1 Computational and experimental conditions

Physical properties and chemical properties are absolutely important to the reaction system.
Table 1, Table 2 and Table 3 give the constituents, chemical composition and thermal physical properties of basalt concrete respectively [4].

Computed cases are chosen from HEDL small scale test S1[5], medium scale test SC20[4] and large scale test LFT6[6]. Experimental conditions are listed in Table 4.

Table 1 Constituent of basalt concrete

Constituent	Content / $kg \cdot m^{-3}$
Concrete	293
Sand	872
Aggregate	1070
Water	146
Water-reducing agent	0.71
Air absorbent	0.15

Table 2 Chemical composition of basalt concrete

Composition	Weight percent / %
SiO_2	51.4
Al_2O_3	11.3
CaO	12.9
MgO	3.0
FeO	2.1
Fe_2O_3	5.3
TiO_2	1.7
Na_2O	2.4
K_2O	1.43
S	0.02
SO_4	0.20
CO_2	0.57
Total	92.32

Table 3 Thermal physical and chemical properties

Parameter	SiO_2	H_2O	Na	H_2	NaOH	$NaSiO_3$
W	60.0	18.0	23	2.0	40.0	122
P^*	0	1.758×10^{10}	3.27×10^{9}	0	0	0
T^*	0	4.50×10^{3}	1.202×10^{4}	0	0	0
L	0	2.335×10^{6}	3.909×10^{6}	0	0	0
H_f	-8.577×10^{8}	-2.858×10^{8}	0	0.	-4.259×10^{8}	-1.556×10^{9}
H_{fg}	0	2.33×10^{6}	3.87×10^{6}	0	0	0
T_m	1.743×10^{3}	2.730×10^{2}	3.709×10^{2}	0	5.95×10^{2}	1.36×10^{3}
T_s	0	3.73×10^{2}	1.18×10^{3}	0	0	0
c_{Ps}	1.10×10^{3}	4.184×10^{3}	1.296×10^{3}	0	3.83×10^{3}	1.485×10^{3}
c_{Pl}	0	4.184×10^{3}	1.296×10^{3}	0	3.83×10^{3}	0
c_{Pg}	0	4.184×10^{3}	0	1.485×10^{3}	0	0
ρ_s	2.20×10^{3}		0	0	0	0
ρ_l	0	1.476×10^{2}	3.00×10^{2}	0	0	0
ρ_g	0	2.741×10^{-1}	2.802×10^{-1}	2.437×10^{-2}	0	0
K	0.5	0.11	50.0	5.00×10^{-2}	0.50	0.50

Note: All the above parameter's units are of International Standard Unit.

Table 4 Experimental conditions

Test No.	Scale	Concrete		Sodium pool		
		Surface area / m^2	Depth / cm	Mass / kg	Temperature / °C	Heater and thermocouple
S1	Small	0.081	30	1	600	Yes
SC20	Medium	0.093	30	3.6	550	No
LFT6	Large	0.836	61	250	820	Yes

5.2 Computational results and analysis

Fig. 4 and Fig. 5 illustrate the comparison of temperature between analytical results and experimental results for test S1 and test SC20.

Table 5 gives comparison of penetration depth between analytical results and experimental results for test S1 and test SC20.

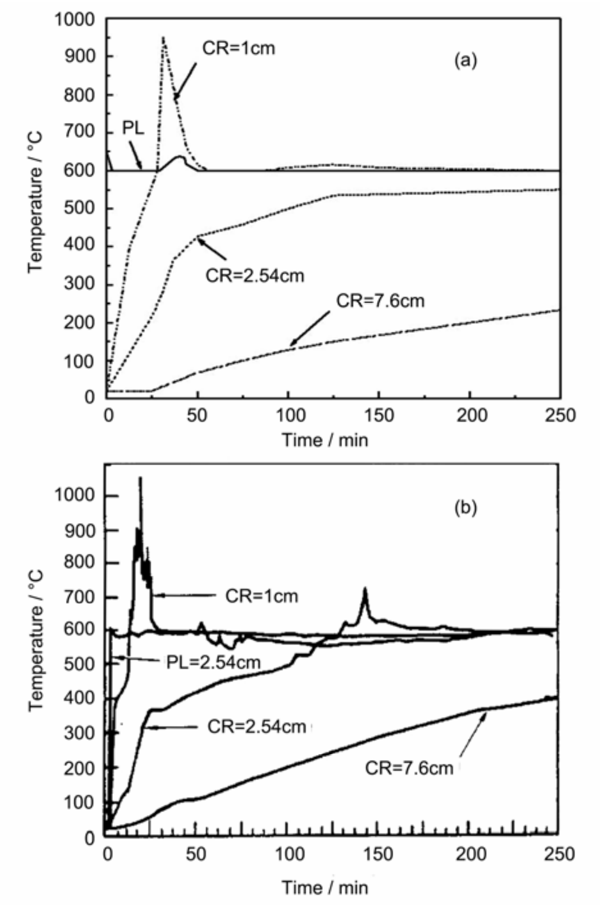

Fig. 4 Comparison of temperature for test S1. (a) Analytical results，(b) Experimental results.

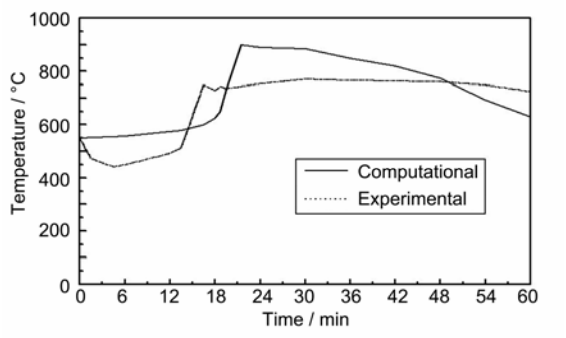

Fig. 5 Comparison of sodium pool temperature.

Table 5 Penetration depth of concrete

Test No.	Measured value / m	Computational values / m
S1	0.042 ± 0.029	0.023
SC20	0.15	0.18

Seen from Table 5, computational values fit well with the experimental values.

Comparison between experimental results and computational ones for test LTF6 is listed in Fig. 6 to Fig. 8.

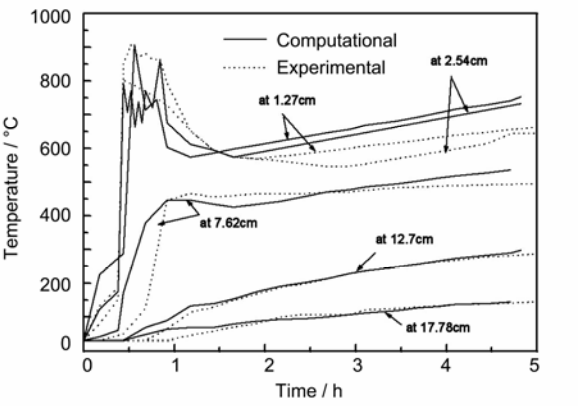

Fig. 6 Comparison between computational and measured temperatures.

As shown in Fig. 6, in the area near thermal surface (from 1.27 cm to 2.54 cm), temperature varies violently. The reason is that the concrete around that area is severely destroyed mechanically, and hence leads to the gradual increase of the gradient of enthalpy of concrete. If we define the period of curve between its ascending and descending as Invalid Reaction Period, we can find that computational values are consistent with experimental data during this period. Three hours after the formation of reactants, the computational value of temperature is a little higher than the measured one. This deviation is due to the neglect of gas transport in the reactant layer during calculation and neglect of swelling of the reactant. At 12.7 cm below the surface, the temperature increases very slowly, which indicates that mechanical damage of surface doesn't extend till here. Only heat conduction from the upper heat areas increases the temperature.

Fig. 7 illustrates the comparison of released amount and released rate of hydrogen between computational and experimental values. There is a peak of released rate at about 0.35 h, which may be attributed to the increment of diffusion flow rate of sodium and increment of released amount of water. The released rate of hydrogen doesn't reduce immediately after the ceasing of mechanical damage. On the contrary, the curve of released rate goes down gradually. This tendency is due to the consistent heating-up of concrete by the chemical reaction energy released in the reaction course. The peak of computational values comes earlier than experimental ones, and it is slightly larger than that of measured ones. All these can be attributed to the neglect of block effect of reactant layer during calculation. However, overall, they fit well.

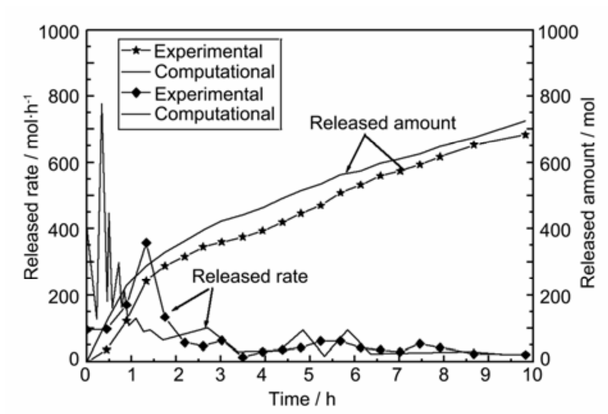

Fig. 7 Variation of released rate and amount of hydrogen.

As is seen from Fig. 8, penetration depth increased rapidly in the early stages. This may be attributed to the mechanical damage of concrete. When this damage ceases, the increase of penetration depth slows down and finally the penetration rate reduces to 0.

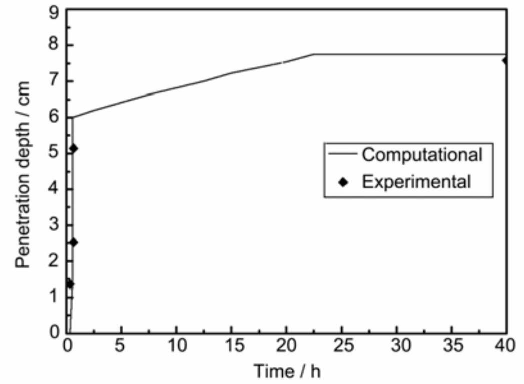

Fig. 8 Comparison of penetration depth between computational and experimental values.

6 Conclusion

Sodium-concrete interaction is a key safety issue in safety analysis of liquid metal cooled fast breeder reactors (LMFBRs). The chemical kinetics model is a key component of the sodium-concrete interaction model. The conservation equations integrated in sodium-concrete interaction model cannot be solved without a set of relationships that couple the equations together. This has to be carried out by the chemical kinetics model.

However, the simulation of chemical kinetics is very difficult due to complexity of the mechanism of chemical reactions between sodium and concrete. This paper tried to simulate the chemical kinetics under certain hypotheses. The chemical kinetics model was integrated with the conservation equations to form a program. Penetration depth, penetration rate, hydrogen flux and reaction heat, etc. could be deduced by this program.

Good agreements of an overall transient behavior were obtained in a series of sodium-concrete interaction experiment analysis. The comparison between analytical and experimental results showed that the chemical kinetics model presented in this paper was creditable and reasonable for simulating the sodium concrete interactions.

References

1 Anttila A S. Sodium concrete ablation model, NUREG/CR-2029, SAND81-0145.R7, 1981

2 Acton R U. Molten sodium interaction with basalt concrete and siliceous firebrick, SAND79-0938, 1979

3 Deng J Z. Calculation Method (in Chinese), Xi'an: Xi'an Jiaotong University Press, 1985

4 Hassberger J A. Intermediate-scale sodium concrete interaction tests with basalt and limestone concrete, HEDL-TME 79-55, Hanford Engineering Development Laboratory, 1981

5 Colburn R P. Sodium concrete reactions, American Nuclear Society, International meeting on fast reactor safety technology, Seattle, Washington, August 19-23, 1979

6 Nguyen D H. Sodium concrete interaction model development, Actes De La Conference De Lyon, Proc. LMFBR Safety Topical Meeting, Lyon Ecully, France, 1982